LETTER • OPEN ACCESS

Robust Amazon precipitation projections in climate models that capture realistic land–atmosphere interactions

View the article online for updates and enhancements.

ENVIRONMENTAL RESEARCH
LETTERS

LETTER

Robust Amazon precipitation projections in climate models that capture realistic land–atmosphere interactions

J C A Baker[1,*] ⬥, L Garcia-Carreras[2] ⬥, W Buermann[3], D Castilho de Souza[4], J H Marsham[1] ⬥, P Y Kubota[4], M Gloor[5] ⬥, C A S Coelho[4] ⬥ and D V Spracklen[1] ⬥

[1] School of Earth and Environment, University of Leeds, Leeds, United Kingdom
[2] Department of Earth and Environmental Sciences, University of Manchester, Manchester, United Kingdom
[3] Institut fuer Geographie, Universitaet Augsburg, D-86135 Augsburg, Germany
[4] Centro de Previsão de Tempo e Estudos Climáticos (CPTEC), Instituto Nacional de Pesquisas Espaciais (INPE), Cachoeira Paulista, SP, Brazil
[5] School of Geography, University of Leeds, Leeds, United Kingdom
* Author to whom any correspondence should be addressed.

E-mail: J.C.Baker@Leeds.ac.uk

Abstract

Land–atmosphere interactions have an important influence on Amazon precipitation (P), but evaluation of these processes in climate models has so far been limited. We analysed relationships between Amazon P and evapotranspiration (ET) in the 5th Coupled Model Intercomparison Project models to evaluate controls on surface moisture fluxes and assess the credibility of regional P projections. We found that only 13 out of 38 models captured an energy limitation on Amazon ET, in agreement with observations, while 20 models instead showed Amazon ET is limited by water availability. Models that misrepresented controls on ET over the historical period projected both large increases and decreases in Amazon P by 2100, likely amplified by unrealistic land–atmosphere interactions. In contrast, large future changes in annual and seasonal-scale Amazon P were suppressed in models that simulated realistic controls on ET, due to modulating land–atmosphere interactions. By discounting projections from models that simulated unrealistic ET controls, our analysis halved uncertainty in basin-wide future P change. The ensemble mean of plausible models showed a robust drying signal over the eastern Amazon and in the dry season, and P increases in the west. Finally, we showed that factors controlling Amazon ET evolve over time in realistic models, reducing climate stability and leaving the region vulnerable to further change.

1. Introduction

The Amazon basin contains the world's largest tropical rainforest, which both depends on, and substantially influences, the regional hydrological cycle (Marengo 2006). Evapotranspiration (ET) from forests is essential for maintaining Amazon climate, ensuring water vapour is replenished during transport across the basin by recycling precipitation (P) back to the atmosphere (Salati *et al* 1979, Eltahir and Bras 1994). Amazon forests are highly dependent on this supply of recycled water (Spracklen *et al* 2012, Staal *et al* 2018), and up to 70% of P in the southern basin originates from terrestrial ET upwind (van der Ent *et al* 2010). Furthermore, it has been suggested

that ET may play a role in Amazon wet season initiation (Wright *et al* 2017). Evidence from *in situ* measurements and moisture-balance analysis indicates that ET is controlled by net radiation over most of the basin (Da Rocha *et al* 2004, Fisher *et al* 2009, Sun *et al* 2019), consistent with satellite studies showing Amazon photosynthesis is not water-limited in areas where annual P exceeds 2000 mm (Guan *et al* 2015).

Understanding how the Amazon water cycle may change under future warming scenarios is crucial for predicting how the forest, and its store of terrestrial carbon, may respond. The Amazon hydrological cycle has become increasingly seasonal since the 1990s (Gloor *et al* 2013), and floods and droughts have become more extreme (Marengo and Espinoza 2016,

Barichivich *et al* 2018). Although vegetation models simulated a relatively stable carbon sink over the Amazon since 1990 (Sitch *et al* 2015), strong P anomalies disrupt carbon sequestration (Gatti *et al* 2014), and ground-based measurements suggest the rate of forest carbon uptake is in decline (Brienen *et al* 2015). Climate change is already impacting the Amazon, therefore, determining the direction of future hydrological changes is imperative.

In general, models from the 5th Coupled Model Intercomparison Project (CMIP5) have struggled to reproduce historical Amazon P (Yin *et al* 2013, Knutson and Zeng 2018), and P projections for the next century are highly uncertain (Christensen *et al* 2013). Although the ensemble mean suggests a modest drying trend over the basin, discrepancies in the direction and magnitude of future changes limit confidence in projections (Boisier *et al* 2015, Chadwick *et al* 2016). When standard model performance metrics are unable to narrow the uncertainty of regional P changes, process-based model evaluation may help to constrain future simulations (Rowell *et al* 2016). Following such a mechanistic approach, inter-model differences in simulated Amazon P have been attributed to factors including spatial variation in sea surface temperature (SST) change and the land–sea temperature contrast (Kent *et al* 2015), the CO_2 physiological effect on stomatal conductance (Skinner *et al* 2017), and strength of the Atlantic meridional overturning circulation (Chen *et al* 2018).

Land–atmosphere interactions are another source of variability between CMIP models (Seneviratne *et al* 2013, Mueller and Seneviratne 2014, Levine *et al* 2016). Models have been shown to misrepresent the strength and direction of Amazon land–atmopshere interactions (Levine *et al* 2016, Baker *et al* 2021a), and struggled to capture controls on Amazon photosynthetic productivity due to overestimation of dry-season water stress (Gentine *et al* 2019, Green *et al* 2020). However, the extent to which land–atmosphere interactions explain differences in Amazon P projections has not yet been explored. Here, we used observations to assess representation of Amazon land–atmosphere interactions in CMIP5 models. Our findings demonstrate that regulation of ET offers an important constraint on the realism of model behaviour. We found that the most extreme P projections (reductions and increases) could be discounted, as these were from models that simulated incorrect controls on ET. Meanwhile, models that captured realistic controls on moisture fluxes showed an ability to buffer regional hydroclimatic changes over the next century.

2. Methods

Relationships between P and ET can be used to diagnose the direction and strength of land–atmosphere interactions, indicating whether ET fluxes are regulated by an atmospheric influence or a land-surface control (figure 1(a)). In regions where ET is controlled by available surface energy, reductions in P (and thus cloudiness, supplementary figure 1 (available online at stacks.iop.org/ERL/16/074002/mmedia)) drive an increase in incoming solar radiation, causing ET to increase. In contrast, areas where ET is water-limited show positive relationships between P and ET, as increases in P drive increasing soil water availability. To categorise Amazon ET as either energy-limited or water-limited, we calculated correlations between monthly anomalies of P and ET from 38 CMIP5 climate models and compared them against observations.

2.1. Data
We obtained global observations of P and ET for an 11 year period (2003–2013). We used a merged satellite-gauge P product (Huffman *et al* 2007) and seven ET products, including three satellite-based datasets, three datasets based on interpolated flux-tower measurements, and a novel reanalysis, to overcome uncertainty in ET over the Amazon (Sörensson and Ruscica 2018, Baker *et al* 2021b). In addition to P and ET, we also analysed cloud cover (CLD), surface radiation (RDN) and soil moisture (SM) to examine model representation of physical processes along the full hydrological pathway. Details of all observational products are provided in table 1, with additional information in the supplementary methods.

Historical simulations from 38 CMIP5 models (supplementary tables 1 and 2) were downloaded at monthly resolution from the Centre for Environmental Data Analysis archive (http://data.ceda.acuk/badc/cmip5/). When available, multiple realisations were used to derive an ensemble mean, else a single run was used. We used data over an 11 year period (1994–2004) to align with observations. There is a discrepancy in the time periods analysed for models and observations (2003–2013). Although land–atmosphere interactions may be expected to evolve over time, as the two periods are separated by less than a decade we do not expect this to have had a substantial impact on our findings. All model simulations and observations were regridded to $1° \times 1°$ resolution using an area-weighted approach to ensure an equal number of Amazon grid cells across datasets.

2.2. Assessing model representation of land–atmosphere interactions
Simultaneous linear P-ET correlations were used to categorise controls on Amazon ET in observations and models. These correlations are not expected to capture the full complexity of land–atmosphere interactions over the Amazon, but rather to provide a broad indication of the direction of influence between the land surface and the atmosphere. Pearson correlation coefficients were computed between monthly
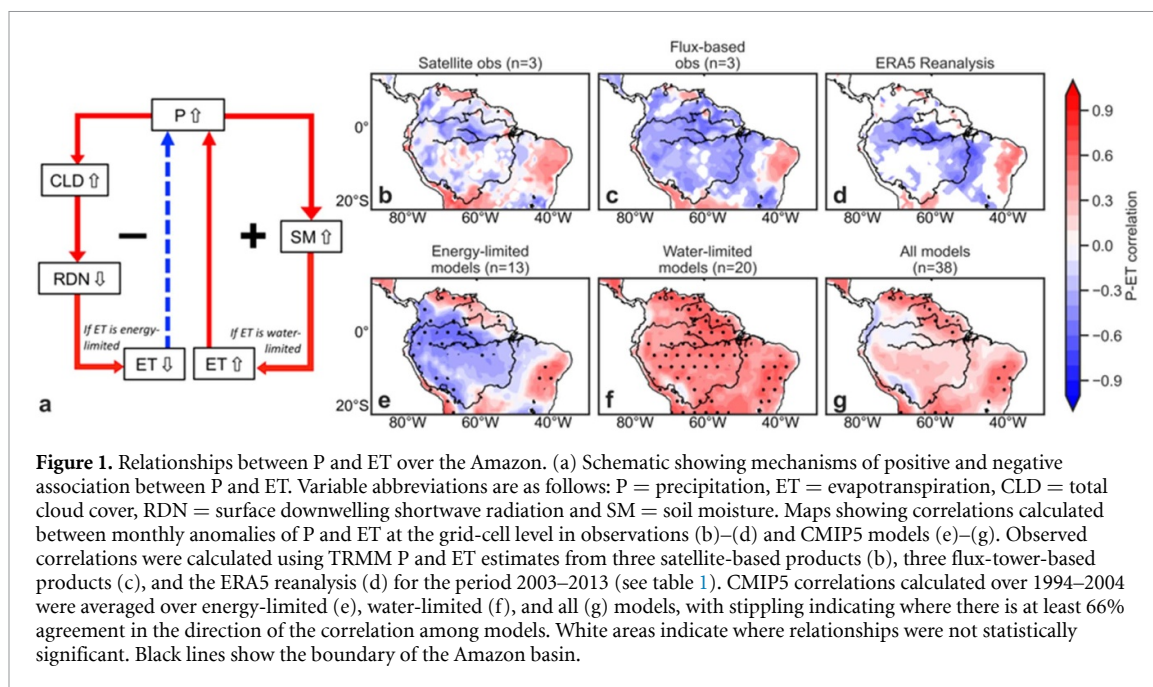
Figure 1. Relationships between P and ET over the Amazon. (a) Schematic showing mechanisms of positive and negative association between P and ET. Variable abbreviations are as follows: P = precipitation, ET = evapotranspiration, CLD = total cloud cover, RDN = surface downwelling shortwave radiation and SM = soil moisture. Maps showing correlations calculated between monthly anomalies of P and ET at the grid-cell level in observations (b)–(d) and CMIP5 models (e)–(g). Observed correlations were calculated using TRMM P and ET estimates from three satellite-based products (b), three flux-tower-based products (c), and the ERA5 reanalysis (d) for the period 2003–2013 (see table 1). CMIP5 correlations calculated over 1994–2004 were averaged over energy-limited (e), water-limited (f), and all (g) models, with stippling indicating where there is at least 66% agreement in the direction of the correlation among models. White areas indicate where relationships were not statistically significant. Black lines show the boundary of the Amazon basin.

Table 1. Observational datasets used in this study.

Variable	Product	Original spatial resolution (°)	Original temporal resolution	Reference
P	TRMM 3B43	0.25	Month	Huffman *et al* (2007)
ET	MODIS MOD16A2	0.05	8 d	Mu *et al* (2007), Mu *et al* (2011)
	P-LSH	0.083	Month	Zhang *et al* (2010)
	GLEAM	0.25	Month	Miralles *et al* (2011), Martens *et al* (2017)
	ERA5	0.25	Month	Dee *et al* (2011)
	WECANN	1.0	Month	Alemohammad *et al* (2017)
	FLUXCOM_RS	1.0	Month	Jung *et al* (2019)
	FLUXCOM_RS + METEO[a]	1.0	Month	Jung *et al* (2019)
CLD fraction	CLARA-A1	0.25	Month	Karlsson *et al* (2013)
Shortwave incoming solar RDN	CLARA-A1	0.25	Month	Karlsson *et al* (2013)
SM	ERA5	0.25	Month	Hersbach *et al* (2020)

[a] Note that following calculation of monthly anomalies this dataset is labelled FLUXCOM_METEO to account for the removal of the remote-sensing-derived signal.

anomalies of P and ET globally at the grid-cell scale for all datasets. Anomalies represent the deviation from the climatological mean and were derived by subtracting the long-term seasonal cycle from the monthly data. To constrain our analysis, we downloaded an Amazon basin shapefile (black boundary shown in figure 1) from observation service SO HYBAM (www.ore-hybam.org) and generated a $1° \times 1°$ mask to identify Amazon grid cells. Datasets were only categorised if at least 25% of Amazon grid cells showed significant P-ET correlations. A *t*-test was used to identify whether the calculated coefficient was statistically different from zero and any dataset

that did not meet this criterion was excluded from the study (1 CMIP5 model). To avoid overstating the significance of our results as a result of multiple-hypothesis testing, we applied a method to control for the false discovery rate, as suggested by Wilks (2016). We used the Benjamini/Hochberg approach (Benjamini and Hochberg 1995) implemented by the 'statmodels' Python package to adjust the *p*-values used to identify the statistical significance of correlations. A binary classification system was applied to eligible datasets, whereby datasets were classed as either water-limited or energy-limited if at least 66% of the significant correlations were positive or negative

respectively. A sensitivity analysis showed that changing the thresholds for categorisation had minimal influence on the overall results, and thus thresholds were selected to balance stringency and dataset retention (supplementary figure 2, supplementary table 3).

In addition to P-ET relationships, correlations were computed between monthly anomalies of other variables to fully assess model representation of physical processes in the Amazon hydrological cycle, including P-CLD, P-SM, RDN-CLD, RDN-P, RDN-ET and SM-ET relationships. We tested how P-ET, RDN-ET and SM-ET relationships responded to spatial variation in P, considering water-limited and energy-limited models separately. Correlation coefficients for all Amazon grid cells were binned by mean annual P, using a bin width of 50 mm. Bins with fewer than five data points were excluded from the analysis.

2.3. Future P projections

We assessed whether differences in model representation of Amazon ET controls influenced Amazon P projections. For this, we used simulations from the representative concentration pathway (RCP) 8.5 experiment, a future-change scenario with high radiative forcing at the end of the century (Riahi *et al* 2011). Change anomalies were calculated at the annual time scale (using data from all months, or three-monthly periods) for 2008–2099, taking 1980–1999 as the historical reference period. Interannual data were smoothed with an 11 year moving average to better visualise inter-decadal trends (Boisier *et al* 2015). Reported end-of-century changes represent the mean P anomaly across the 20 year period from 2080 to 2099 (ΔP). We used a Monte Carlo-type approach to determine whether the standard deviation (σ) in basin-mean ΔP across the 13 energy-limited CMIP5 models was different to what might be expected by chance (supplementary methods 1.4).

To test the hypothesis that the smaller future range in P projections in energy-limited models was influenced by climate buffering due to the negative relationship between P and ET, we examined ΔP together with changes in ET and RDN (ΔET and ΔRDN) at the grid-cell scale by the end of the century (2080–2099), using 1980–1999 as the historical reference period. We calculated linear regression relationships between ΔP and ΔET and between ΔRDN and δET, where δET represents the difference between the actual simulated ΔET in the grid cell, and the ΔET predicted from ΔP using the linear ΔP-ΔET relationship derived from all models, accounting for uncertainty along both axes (York 1966). Relationships were calculated for all, energy-limited and water-limited models, using data from all Amazon grid cells.

3. Results

3.1. Opposite controls on ET in different climate models

Amazon P-ET correlations based on ET estimates from satellites, flux-tower measurements and reanalysis were predominantly negative (figures 1(b)–(d), supplementary figure 3), providing strong evidence that Amazon ET is primarily energy-limited, in agreement with earlier studies (Fisher *et al* 2009, Sun *et al* 2019). All but one of the ET products analysed showed good agreement in the direction of correlations, particularly over the northern Amazon, though there were some spatial differences elsewhere (supplementary figure 4). Furthermore, the single satellite ET product that showed opposing results has previously been shown to perform poorly in the Amazon (Miralles *et al* 2011, Baker *et al* 2021b).

Strikingly, only 13 out of 38 CMIP5 models captured an energy control on Amazon ET (hereafter energy-limited models), while 20 models instead showed Amazon ET was limited by water availability (hereafter water-limited models, supplementary figure 3). The spatial pattern of P-ET relationships in energy-limited models matched well with observations, particularly in the northwest Amazon where there was good agreement among models (figure 1(e), supplementary figure 4). In contrast, water-limited models showed positive P-ET correlations over the whole basin (figure 1(f)). Given that nearly half of CMIP5 models simulated the wrong controls on Amazon moisture fluxes, the multi-model ensemble provides a poor representation of the observed state (figure 1(g)). Trying to understand future changes in Amazon hydrology through an assessment of the ensemble mean is therefore unlikely to yield reliable results. The division of CMIP5 models into two populations with opposing controls on Amazon ET was supported by a Budyko drought-index analysis, whereby the ratio of potential ET (PET) to P indicates an energy-limited (PET/P < 1) or water-limited (PET/P > 1) evaporative regime (supplementary methods 1.2, supplementary figure 5). Together, these results highlight a potential source of divergence in simulations of the Amazon hydrological cycle among CMIP5 models. Finally, we repeated our analysis using newly-available historical simulations from 26 CMIP6 models and found consistent results (supplementary figure 6), indicating that our findings from CMIP5 are generalizable to the latest generation of climate models.

3.2. Response of ET controls to spatial and temporal P variation

Land–atmosphere interactions in CMIP5 models can be modulated by background P (Berg and Sheffield 2018), so we tested whether differences in P could
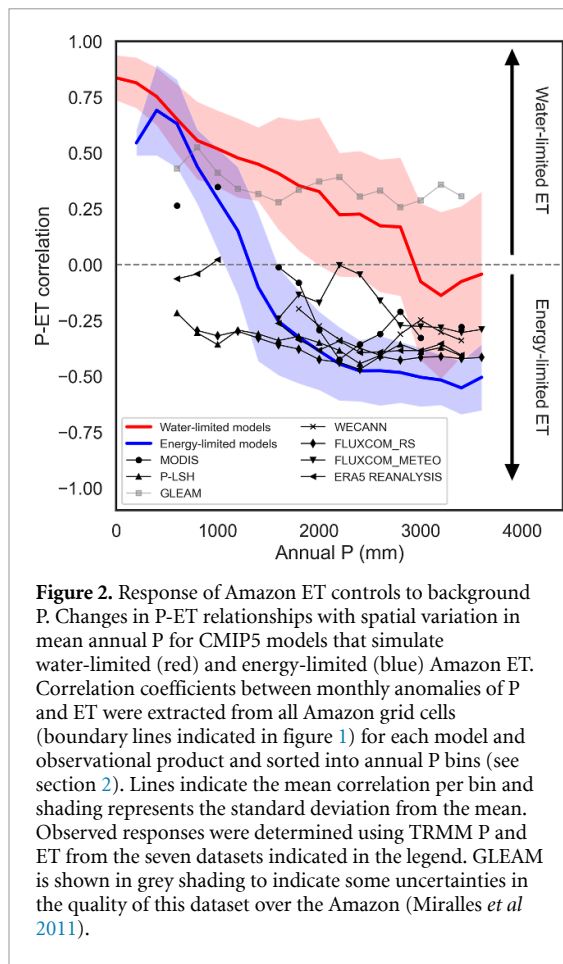
Figure 2. Response of Amazon ET controls to background P. Changes in P-ET relationships with spatial variation in mean annual P for CMIP5 models that simulate water-limited (red) and energy-limited (blue) Amazon ET. Correlation coefficients between monthly anomalies of P and ET were extracted from all Amazon grid cells (boundary lines indicated in figure 1) for each model and observational product and sorted into annual P bins (see section 2). Lines indicate the mean correlation per bin and shading represents the standard deviation from the mean. Observed responses were determined using TRMM P and ET from the seven datasets indicated in the legend. GLEAM is shown in grey shading to indicate some uncertainties in the quality of this dataset over the Amazon (Miralles *et al* 2011).

nearly 3000 mm yr^{-1}, suggesting they fail to accurately represent the physical processes that modulate ET over the Amazon.

Models also exhibited differences in behaviour in response to temporal variation in P. Although all models simulated Amazon P seasonality relatively well (supplementary figure 8), energy-limited models reproduced a strong seasonal cycle in P-ET correlations, as shown in observations, while water-limited models showed little variation in P-ET correlations throughout the year (supplementary figure 9). Energy-limited models showed a clear pattern of behaviour with varying water availability, simulating negative P-ET correlations in months where mean Amazon P exceeded 200 mm month^{-1} (November–April) and positive P-ET correlations in the driest part of the year (July–September). Meanwhile, water-limited models simulated positive P-ET correlations in all months, including months where simulated Amazon P was greater than 200 mm month^{-1} (December–March). These results, together with the results presented in figure 2, demonstrate that although differences in background P may explain some of the differences between energy and water-limited models, there also appears to be a more fundamental difference in model behaviour between the two groups in their ability to respond to changing background conditions. Since controls on ET may evolve with changing climate, capturing a switch in ET controls with changing P has implications for future projections.

3.3. Tracing relationships along the full hydrological pathway

To better understand the physical processes causing differences in behaviour among climate models, we evaluated relationships along the full hydrological pathway (figure 3). Both groups of models generally captured relationships between variables in the two branches of figure 1(a), with the exception of correlations between RDN and ET, and between SM and ET. Water-limited models tended to underestimate and overestimate RDN-ET and SM-ET relationship strengths respectively, relative to those seen in observations and energy-limited models (figure 3, supplementary figures 10 and 11). We found SM-ET correlations in the two model populations showed divergent responses to increasing annual P that were comparable to the responses of P-ET relationships, while RDN-ET correlations showed more similar behaviour (figure 2, supplementary figure 12). This result suggests that models differ in their ability to represent realistic P-ET correlations over the Amazon due to differences in processes related to the soil-plant-atmosphere moisture-transport pathway, highlighting an area for future model development.
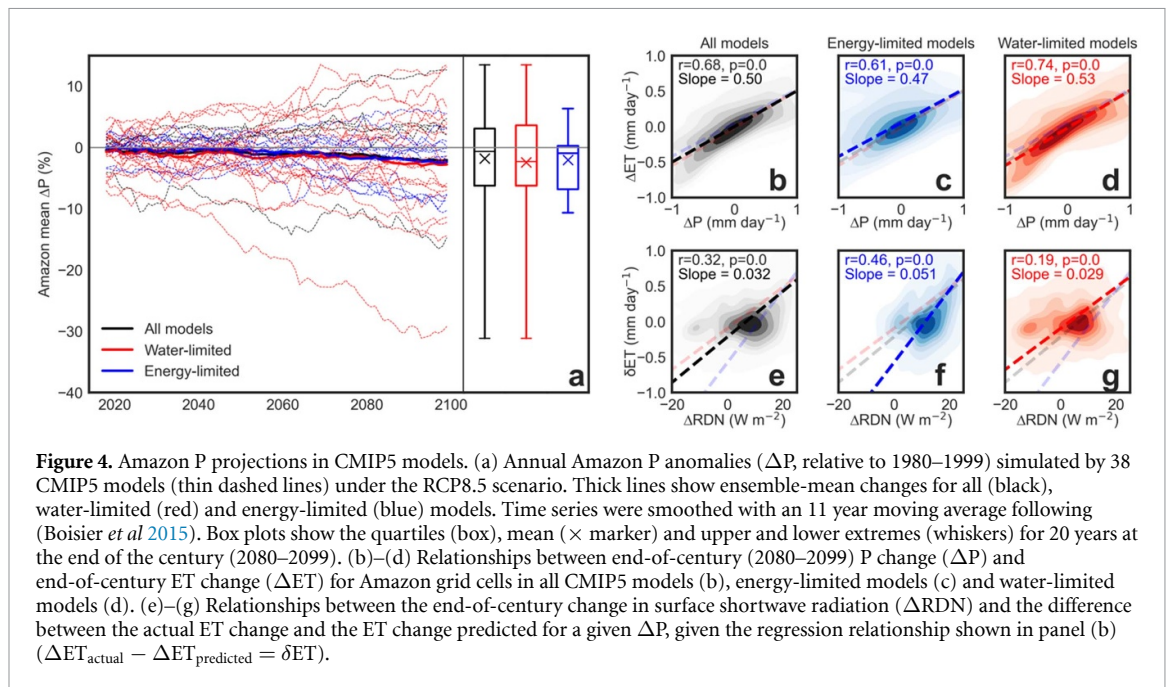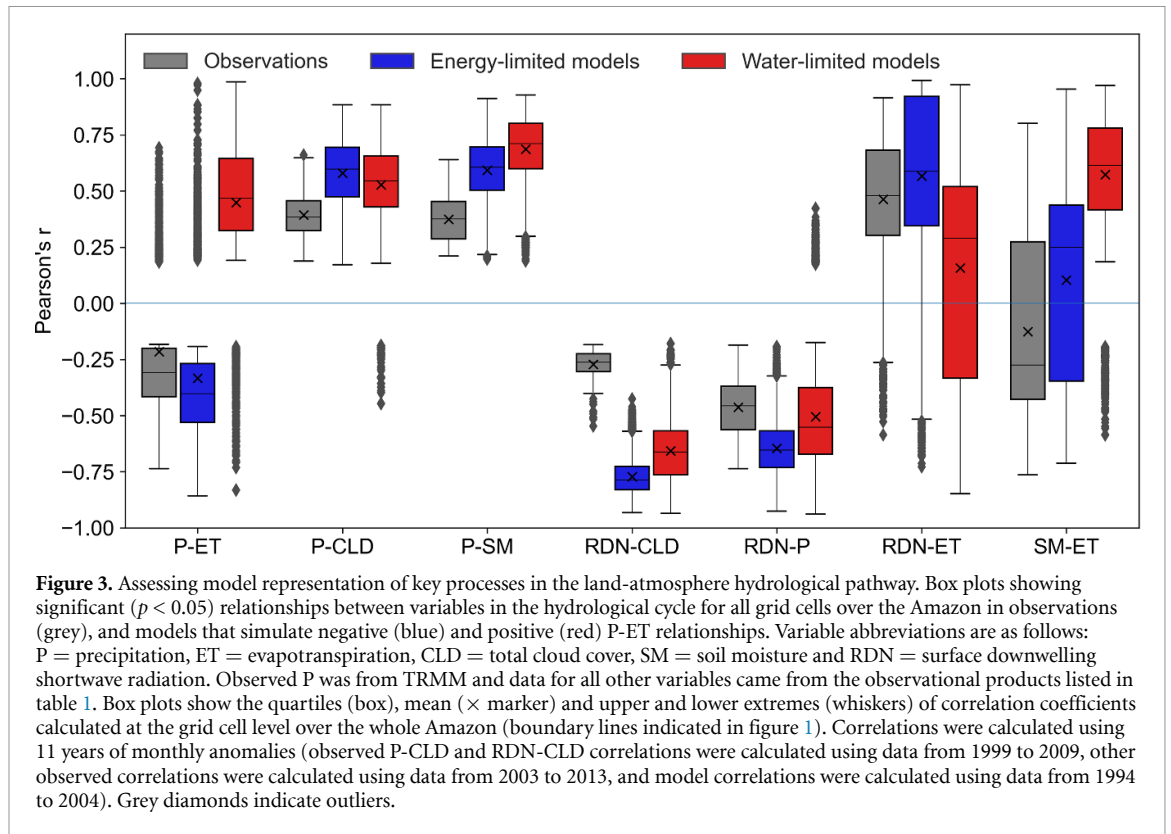
explain differences in ET controls between the two model populations. Models that captured an energy limitation on Amazon ET tended to be wetter over the whole Amazon, and simulated mean annual P closer to observations (supplementary figure 7). The five wettest models were all energy-limited, suggesting that simulating a sufficiently high background Amazon P may be a first step towards capturing the right controls on ET. However, there were exceptions to this pattern, with some drier models still simulating a radiation control on Amazon ET, and wetter models where ET was found to be water-limited. When we examined how P-ET relationships responded to spatial variation in P, we found that energy and water-limited models simulated opposite controls on ET over the same range in P (figure 2). Models in the energy-limited population showed a relatively sharp transition from positive to negative P-ET correlation coefficients when P reached around 1500 mm yr^{-1}, followed by a more gradual decline in correlation as annual P continued to rise (figure 2). This behaviour, which is supported by the majority of observations (figure 2), is consistent with hydrological theory (Budyko 1974), and our current understanding of the controls on Amazon photosynthesis (Guan *et al* 2015). In contrast, water-limited models showed positive P-ET correlations until P reached

Figure 3. Assessing model representation of key processes in the land-atmosphere hydrological pathway. Box plots showing significant ($p < 0.05$) relationships between variables in the hydrological cycle for all grid cells over the Amazon in observations (grey), and models that simulate negative (blue) and positive (red) P-ET relationships. Variable abbreviations are as follows: P = precipitation, ET = evapotranspiration, CLD = total cloud cover, SM = soil moisture and RDN = surface downwelling shortwave radiation. Observed P was from TRMM and data for all other variables came from the observational products listed in table 1. Box plots show the quartiles (box), mean (× marker) and upper and lower extremes (whiskers) of correlation coefficients calculated at the grid cell level over the whole Amazon (boundary lines indicated in figure 1). Correlations were calculated using 11 years of monthly anomalies (observed P-CLD and RDN-CLD correlations were calculated using data from 1999 to 2009, other observed correlations were calculated using data from 2003 to 2013, and model correlations were calculated using data from 1994 to 2004). Grey diamonds indicate outliers.

Figure 4. Amazon P projections in CMIP5 models. (a) Annual Amazon P anomalies (ΔP, relative to 1980–1999) simulated by 38 CMIP5 models (thin dashed lines) under the RCP8.5 scenario. Thick lines show ensemble-mean changes for all (black), water-limited (red) and energy-limited (blue) models. Time series were smoothed with an 11 year moving average following (Boisier *et al* 2015). Box plots show the quartiles (box), mean (× marker) and upper and lower extremes (whiskers) for 20 years at the end of the century (2080–2099). (b)–(d) Relationships between end-of-century (2080–2099) P change (ΔP) and end-of-century ET change (ΔET) for Amazon grid cells in all CMIP5 models (b), energy-limited models (c) and water-limited models (d). (e)–(g) Relationships between the end-of-century change in surface shortwave radiation (ΔRDN) and the difference between the actual ET change and the ET change predicted for a given ΔP, given the regression relationship shown in panel (b) ($\Delta ET_{actual} - \Delta ET_{predicted} = \delta ET$).

3.4. Constraining future Amazon P projections

By identifying models that were able to correctly reproduce key land–atmosphere interactions in the historical period, we could constrain future projections of Amazon P. Models that correctly captured an energy limitation on Amazon ET showed a highly constrained future P response when compared to water-limited models (figure 4(a)). The standard deviation in end-of-century ΔP values was halved in energy-limited models ($\sigma = 4.35$ vs 9.25%, representing a 53% difference), and smaller than expected by chance (estimated through repeated random selection of 13 models from the pool of 38 models, supplementary figure 13). Removal of the water-limited model with the most negative ΔP response (CanEMS2), caused only a slight reduction to the difference in spread between the two model groups ($\sigma = 4.35$ vs 7.01%, representing a 38% difference),

suggesting our results are relatively robust. The water-limited models showed lower coherence in P trends, tending to predict more extreme changes, both positive and negative, in Amazon P than energy-limited models (figure 4(a)). This difference in behaviour can be understood by considering the sign of relationships between P and ET in the two model groups (figure 1(a)). Water-limited models showed a positive correlation between monthly anomalies of P and ET, so any increase (or decrease) in P is likely to be further enhanced, making simulation of extreme changes more likely. On the other hand, energy-limited models had a negative correlation between P and ET, such that Amazon climate will tend to show a buffered response to change. We tested whether this mechanism operated on climate-change timescales through examining climate anomalies at the end of century (ΔP, ΔET and ΔRDN). ΔET was strongly positively related to ΔP across all models (figures 4(b)–(d)), showing the net response of the coupled land-atmosphere system across energy-limited and water-limited models is to simulate increasing ET with increasing P under climate change (and vice versa). However, the greater correlation ($r = 0.74$ vs 0.61) and steeper slope (0.53 vs 0.47) in models where ET is water-limited is indicative of a greater role of ΔP in determining ΔET in the climate change response of these models. More significantly, the difference between the actual simulated ΔET change per Amazon grid cell and the change predicted from grid-cell level ΔP using the all-model regression relationship ($\Delta ET_{actual} - \Delta ET_{predicted} = \delta ET$) was shown to be almost twice as strongly influenced by ΔRDN in models that captured an energy limitation on Amazon ET over the historical period, compared with those that simulated a water limitation (slope = 0.051 vs 0.029 mm d^{-1}/W m^{-2}), with much greater correlation between ΔRDN and δET in energy-limited models ($r = 0.46$ vs 0.19; figures 4(f) and (g)). Thus, ΔRDN modulates the climate-change response in energy-limited models such that for a given value of ΔP, energy-limited (water-limited) models will show a smaller (larger) ΔET response, thus dampening (amplifying) the P anomaly.

We examined whether variation in model set-up might contribute to the observed differences in P projections between the two model populations (supplementary table 1). Dynamic vegetation (simulation of changes in vegetation types in response to climate) was more common among water-limited models than energy-limited models (55 vs 23%, $p = 0.070$, chi-squared statistic), consistent with a recent study showing dynamic global vegetation models generally struggle to capture radiation controls on productivity in tropical regions (O'Sullivan *et al* 2020). However, inclusion of dynamic vegetation had no clear influence on the direction or magnitude of ΔP

(supplementary figure 14), and therefore did not contribute to the observed differences between water-limited and energy-limited CMIP5 models. We also compared model inclusion of the CO_2 physiological effect, where plants reduce their stomatal conductance in response to increased atmospheric CO_2, but the frequency of this feature among the two model groups was similar (76 vs 65% of water-limited models, $p = 0.21$). Likewise, there was no difference in the proportion of energy-limited and water-limited models that included future land-use-change forcing (76 vs 70%, $p = 0.66$). Only four CMIP5 models simulated a nitrogen limitation on photosynthesis and these were all energy-limited models (supplementary table 2). However, given the small number of models including this process (albeit a third of all energy-limited models), we hesitate to draw definite conclusions about the role of nitrogen limitation in influencing ET controls.

Spatial patterns in ΔP were more distinctive in energy-limited models, which simulated annual drying of up to 26% ($\Delta P_{absolute} = -1.3$ mm d^{-1}) over the eastern Amazon, and wetting in the west (<23%, 1.8 mm d^{-1}, figure 5(a)), with at least 75% agreement among models in the direction of change (supplementary figure 15). ΔET maps showed a similar dipole response (supplementary figure 16). Meanwhile, P changes in water-limited models were comparably weaker and more uncertain (drying <13%, wetting <16%, figure 5(b), supplementary figure 15).

Analysis of seasonal ΔP changes provided further evidence for a difference in climate-buffering capability between model populations. Water-limited models, which showed higher and less realistic seasonal P variability over the historical period, simulated stronger increases in seasonality over the next century than energy-limited models (figure 5(c)). However, though smaller in magnitude, the increase in P seasonality was actually more robust in energy-limited models, due to the smaller spread in projections (figure 5(d)). Basin-mean P reductions in energy-limited models were concentrated in the dry season (July–September) and the start of the wet season (October–December), with marginal P increases at other times of the year (supplementary figure 17). The dry season response was particularly striking, with energy-limited models unanimously showing a drying by the end of the century (basin-mean $\Delta P \pm \sigma = -14.3 \pm 6.5$ vs $-14.9 \pm 26.8\%$ in water-limited models; supplementary figure 17), and P reductions of up to 50% over some areas of the eastern Amazon (supplementary figure 18). Overall, these results show that discounting models with unrealistic land–atmosphere interactions revealed more robust future P changes over the Amazon than projected by the full model ensemble, thus substantially reducing uncertainty in future Amazon P.
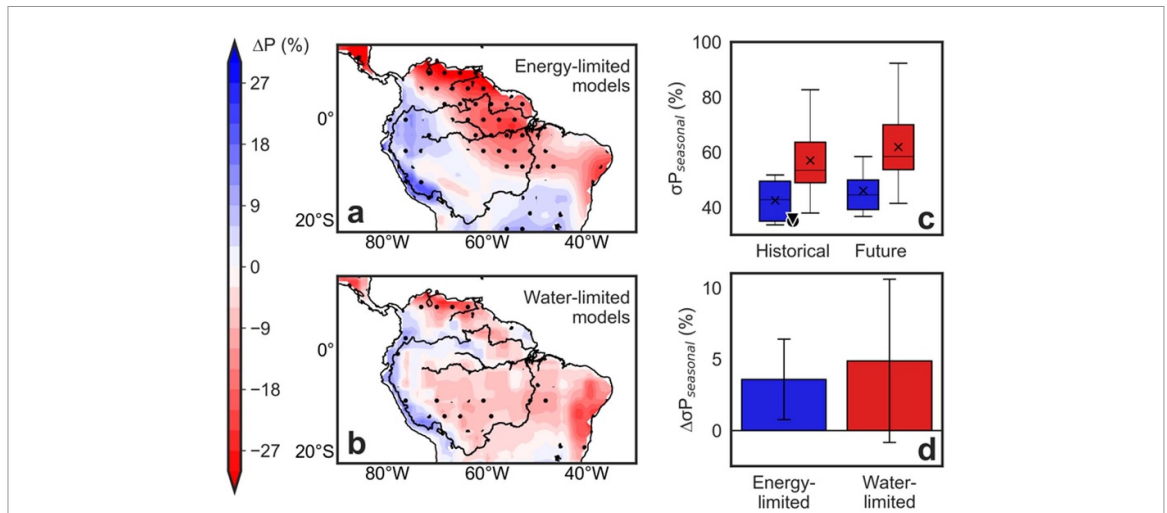
Figure 5. End-of-century P changes in CMIP5 models. Maps show annual P anomalies (ΔP) in energy-limited (a) and water-limited (b) models, calculated as the difference between the 2080–2099 mean and the 1980–1999 mean and expressed as a percentage of historical P (1980–1999). Stippling indicates where there is at least 66% agreement in the ΔP direction among models. Black lines indicate the boundary of the Amazon basin. (c) Standard deviation (σ) of the climatological seasonal cycle in Amazon-mean P (σP$_{seasonal}$) over historical (1980–1999) and future (2080–2099) time periods in energy-limited (blue boxes) and water-limited (red boxes) CMIP5 models. Values are expressed as a percentage of annual P. Box plots show the quartiles (box), mean ($\times$ marker) and upper and lower extremes (whiskers). σP$_{seasonal}$ of historical P from CRU (black circle) and GPCC (black triangle) are also indicated. (d) End-of-century change in σP$_{seasonal}$ ($\Delta\sigma$P$_{seasonal}$), calculated as future σP$_{seasonal}$ minus historical σP$_{seasonal}$, in the two groups of CMIP5 models. Error bars indicate the standard deviation among models in each group.
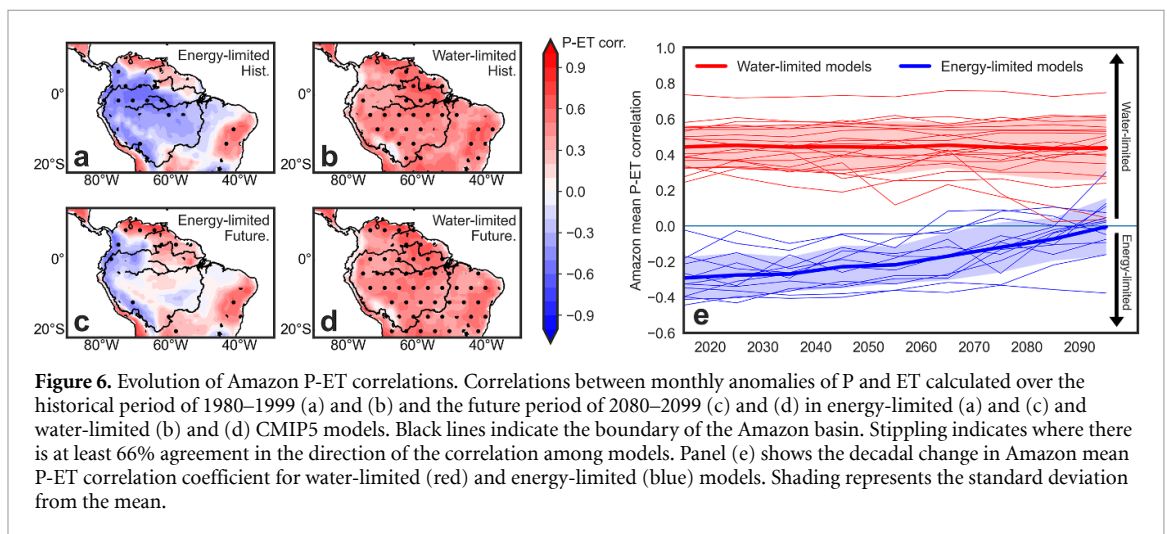
Figure 6. Evolution of Amazon P-ET correlations. Correlations between monthly anomalies of P and ET calculated over the historical period of 1980–1999 (a) and (b) and the future period of 2080–2099 (c) and (d) in energy-limited (a) and (c) and water-limited (b) and (d) CMIP5 models. Black lines indicate the boundary of the Amazon basin. Stippling indicates where there is at least 66% agreement in the direction of the correlation among models. Panel (e) shows the decadal change in Amazon mean P-ET correlation coefficient for water-limited (red) and energy-limited (blue) models. Shading represents the standard deviation from the mean.

3.5. Evolution of land–atmosphere interactions

Energy-limited models, in which controls on ET showed realistic sensitivity to spatial and temporal variation in P (figure 2, supplementary figure 9), showed a shift in land–atmosphere interactions in response to future changes in climate (figure 6). Amazon ET becomes increasingly water-limited by the end of the century, which will reduce the buffering capacity of the climate system. In contrast, water-limited models showed no change in P-ET correlations, consistent with their limited responsiveness to changing background conditions over the historical period (figure 2, supplementary figure 9). The dynamic behaviour displayed by energy-limited models in response to changing water availability illustrates why process-based model evaluation is fundamental to assessments of model performance and highlights the fact that, despite the stabilising mechanism of an inverse P-ET relationship, the Amazon hydrological cycle remains vulnerable to the impacts of climate change.

4. Discussion

Doubts over the direction of Amazon P projections (Christensen *et al* 2013, Chadwick *et al* 2016) have made it difficult for policymakers to plan climate-change mitigation and adaptation strategies. Focussing on model representation of land–atmosphere interactions, a known source of uncertainty over South America (Levine *et al* 2016), we found that models able to reproduce controls on Amazon ET

projected a narrower range of basin-wide P changes by 2100, due to the modulating influence of land–atmosphere interactions on the future P response to climate change. Our analysis halved the uncertainty in end-of-century P projections, while simultaneously revealing a robust drying signal over the eastern Amazon, and wetting in the west. Previous studies have observed a dipole in CMIP5 P projections over South America (Duffy *et al* 2015, Skinner *et al* 2017). It is understood that a reduction in ET in the eastern Amazon causes a warming, drying and deepening of the boundary layer, suppression of convection in the east, and a greater westward transfer of water vapour, which rains out over the Andes and far-western Amazon (Langenbrunner *et al* 2019). Our findings are consistent with this mechanism, and provide additional understanding by offering more certainty on the direction of change.

Earlier efforts using different performance metrics to determine if the Amazon will become wetter or drier also found drying concentrated over the eastern Amazon in constrained projections (Boisier *et al* 2015, Chen *et al* 2018). Furthermore, eight out of ten models identified as having good representation of Atlantic SSTs, which impact Amazon P through location of the intertropical convergence zone (Chen *et al* 2018), overlap with models that captured the correct controls on Amazon ET in this study. This demonstrates that a subset of CMIP5 models are consistently performing well over the Amazon, through accurate representation of different physical processes operating at different spatial scales. This provides further evidence that a 'model democracy' approach, whereby information from all models is combined without discrimination, may not always be the most useful (Eyring *et al* 2019).

Previously identified as a potential 'tipping element' in the Earth's climate system (Lenton *et al* 2008), the fate of the Amazon rainforest has global importance. Of particular interest is whether the Amazon will see a widespread 'dieback', as suggested by an early study (Cox *et al* 2004). Although the likelihood of such an extreme scenario unfolding has been questioned (Malhi *et al* 2009, Rammig *et al* 2010), increases in dry season severity could still threaten the stability of the Amazon forest (Zemp *et al* 2017). We found that while the most extreme increases and decreases in basin-mean Amazon P were from models that simulated unrealistic hydrological relationships, projections from plausible models showed a robust increase in Amazon P seasonality, with P reductions in the dry season and start of the wet season. Increases in the severity and length of the Amazon dry season since the 1970s have already been observed (Fu *et al* 2013, Arias *et al* 2015, Debortoli *et al* 2015), possibly related to changes in land cover (Costa and Pires 2010, Alves *et al* 2017). Projected dry season P reductions in realistic models were comparable to the P anomalies observed during recent major Amazon droughts (i.e. <50%, Marengo *et al* 2008, Coelho *et al* 2012, Marengo and Espinoza 2016), with profound implications for forest dynamics and the terrestrial carbon balance (Gatti *et al* 2014, Feldpausch *et al* 2016). Future declines in P are also expected to impact the Amazon ecosystem, which has already seen a shift in species composition towards those better adapted to survive drought (Esquivel-Muelbert *et al* 2019).

5. Conclusion

Our analysis found that half of all CMIP5 models misrepresent controls on Amazon ET, and show little change in evaporative regime with changing water availability. These models simulated both large increases and decreases in Amazon P by 2100, likely enhanced by unrealistic positive land–atmosphere interactions. In contrast, models showing realistic hydrological behaviour over the historical period showed a more constrained future rainfall response at the basin scale, robust drying in the eastern Amazon and in the dry season, and wetting in the western Amazon, with more than 75% of models agreeing on the direction of these changes. Future work should extend this analysis to other tropical regions, which tend to be less well studied than Amazonia. Altogether, the results presented in this study substantially reduce uncertainty in Amazon P projections, and highlight the vulnerability of the Amazon under an extreme warming scenario.

Data availability

The data that support the findings of this study are openly available in the following repositories:

- CMIP5 model output: http://data.ceda.acuk/badc/cmip5/data/cmip5/output1
- TRMM P: https://disc2.gesdisc.eosdis.nasa.gov/data/TRMM_L3/TRMM_3B43.7/
- MODIS ET: https://search.earthdata.nasa.gov/search/granules?p=C1000000524-LPDAAC_ECS&tl=1554219774!4!!&q=modis%20mod16&ok=modis%20mod16&ac=true
- GLEAM ET: www.gleam.eu/#downloads
- P-LSH ET: http://files.ntsg.umt.edu/data/ET_global_monthly/Global_8kmResolution/
- ERA5 ET and SM: https://climate.copernicus.eu/climate-reanalysis
- WECANN ET: https://avdc.gsfc.nasa.gov/pub/data/project/WECANN/
- FLUXCOM_RS and FLUXCOM_RS_METEO ET: www.bgc-jena.mpg.de/geodb/projects/Data.php
- CLARA-A1 CLD and RDN: https://wui.cmsaf.eu/safira/action/viewDoiDetails?acronym=CLARA_AVHRR_V001
- The data that support the findings of this study are openly available at the following URL/DOI: https://esgf-data.dkrz.de/projects/esgf-dkrz/.

Acknowledgments

Conflict of interest

Code availability

All Python scripts associated with this manuscript are available from the authors upon request.

Author contributions

J C A B, L G C, W B, J H M, M G and D V S devised the study, planned the analysis and discussed the results. J C A B performed the analysis and wrote the paper. All authors provided feedback on the manuscript.

ORCID iDs

J C A Baker ● https://orcid.org/0000-0002-3720-4758

L Garcia-Carreras ● https://orcid.org/0000-0002-9844-3170

J H Marsham ● https://orcid.org/0000-0003-3219-8472

M Gloor ● https://orcid.org/0000-0002-9384-6341

C A S Coelho ● https://orcid.org/0000-0002-9695-5113

D V Spracklen ● https://orcid.org/0000-0002-7551-4597

References

Alemohammad S H, Fang B, Konings A G, Aires F, Green J K, Kolassa J, Miralles D, Prigent C and Gentine P 2017 Water, energy, and carbon with artificial neural networks (WECANN): a statistically-based estimate of global surface turbulent fluxes and gross primary productivity using solar-induced fluorescence *Biogeosciences* **14** 4101–24

Alves L M, Marengo J A, Fu R and Bombardi R J 2017 Sensitivity of Amazon regional climate to deforestation *Am. J. Clim. Change* **6** 75–98

Arias P A, Fu R, Vera C and Rojas M 2015 A correlated shortening of the North and South American monsoon seasons in the past few decades *Clim. Dyn.* **45** 3183–203

Baker J C A, Castilho de Souza D, Kubota P, Buermann W, Coelho C A S, Andrews M B, Gloor M, Garcia-Carreras L, Figueroa S N and Spracklen D V 2021a An assessment of land-atmosphere interactions over South America using satellites, reanalysis and two global climate models *J. Hydrometeorol.* 22 905–22

Baker J C A, Garcia-Carreras L, Gloor M, Marsham J H, Buermann W, Da Rocha H R, Nobre A D, de Araujo A C and

Spracklen D V 2021b Evapotranspiration in the Amazon: spatial patterns, seasonality and recent trends in observations, reanalysis and climate models *Hydrol. Earth Syst. Sci.* 25 2279–300

Barichivich J, Gloor E, Peylin P, Brienen R J W, Schöngart J, Espinoza J C and Pattnayak K C 2018 Recent intensification of Amazon flooding extremes driven by strengthened Walker circulation *Sci. Adv.* **4** eaat8785

Benjamini Y and Hochberg Y 1995 Controlling the false discovery rate: a practical and powerful approach to multiple testing *J. R. Stat. Soc. Ser. B* **57** 289–300

Berg A and Sheffield J 2018 Soil moisture–evapotranspiration coupling in CMIP5 models: relationship with simulated climate and projections *J. Clim.* **31** 4865–78

Boisier J P, Ciais P, Ducharne A and Guimberteau M 2015 Projected strengthening of Amazonian dry season by constrained climate model simulations *Nat. Clim. Change* **5** 656–60

Brienen R J W *et al* 2015 Long-term decline of the Amazon carbon sink *Nature* **519** 344–8

Budyko M 1974 *Climate and Life* (New York: Academic)

Chadwick R, Good P, Martin G and Rowell D P 2016 Large rainfall changes consistently projected over substantial areas of tropical land *Nat. Clim. Change* **6** 177

Chen Y, Langenbrunner B and Randerson J T 2018 Future drying in Central America and northern South America linked with Atlantic meridional overturning circulation *Geophys. Res. Lett.* **45** 9226–35

Christensen J H *et al* 2013 Climate phenomena and their relevance for future regional climate change *Climate Change 2013: The Physical Science Basis. Contribution of Working Group I to the Fifth Assessment Report of the Intergovernmental Panel on Climate Change* ed T F Stocker, D Qin, G-K Plattner, M Tignor, S K Allen, J Boschung, A Nauels, Y Xia, V Bex and P M Midgley (Cambridge: Cambridge University Press) 1217–308

Coelho C A S, Cavalcanti I A F, Costa S M S, Freitas S R, Ito E R, Luz G, Santos A F, Nobre C A, Marengo J A and Pezza A B 2012 Climate diagnostics of three major drought events in the Amazon and illustrations of their seasonal precipitation predictions *Meteorol. Appl.* **19** 237–55

Costa M H and Pires G F 2010 Effects of Amazon and Central Brazil deforestation scenarios on the duration of the dry season in the arc of deforestation *Int. J. Climatol.* **30** 1970–9

Cox P M, Betts R A, Collins M, Harris P P, Huntingford C and Jones C D 2004 Amazonian forest dieback under climate-carbon cycle projections for the 21st century *Theor. Appl. Climatol.* **78** 137–56

Da Rocha H R, Goulden M L, Miller S D, Menton M C, Pinto L D V O, de Freitas H C and Silva Figueira A M 2004 Seasonality of water and heat fluxes over a tropical forest in eastern Amazonia *Ecol. Appl.* **14** 22–32

Debortoli N S, Dubreuil V, Funatsu B, Delahaye F, de Oliveira C H, Rodrigues-Filho S, Saito C H and Fetter R 2015 Rainfall patterns in the Southern Amazon: a chronological perspective (1971–2010) *Clim. Change* **132** 251–64

Dee D, Uppala S, Simmons A, Berrisford P, Poli P, Kobayashi S, Andrae U, Balmaseda M, Balsamo G and Bauer P 2011 The ERA-Interim reanalysis: configuration and performance of the data assimilation system *Q. J. R. Meteorol. Soc.* **137** 553–97

Duffy P B, Brando P, Asner G P and Field C B 2015 Projections of future meteorological drought and wet periods in the Amazon *Proc. Natl Acad. Sci.* **112** 13172–7

Eltahir E A and Bras R L 1994 Precipitation recycling in the Amazon basin *Q. J. R. Meteorol. Soc.* **120** 861–80

Esquivel-Muelbert A *et al* 2019 Compositional response of Amazon forests to climate change *Glob. Change Biol.* **25** 39–56

Eyring V *et al* 2019 Taking climate model evaluation to the next level *Nat. Clim. Change* **9** 102–10

Feldpausch T R *et al* 2016 Amazon forest response to repeated droughts *Glob. Biogeochem. Cycles* **30** 964–82

Fisher J B *et al* 2009 The land-atmosphere water flux in the tropics *Glob. Change Biol.* **15** 2694–714

Fu R *et al* 2013 Increased dry-season length over southern Amazonia in recent decades and its implication for future climate projection *Proc. Natl Acad. Sci.* **110** 18110–5

Gatti L, Gloor M, Miller J, Doughty C, Malhi Y, Domingues L, Basso L, Martinewski A, Correia C and Borges V 2014 Drought sensitivity of Amazonian carbon balance revealed by atmospheric measurements *Nature* **506** 76–80

Gentine P, Massmann A, Lintner B R, Hamed Alemohammad S, Fu R, Green J K, Kennedy D and Vilà-Guerau de Arellano J 2019 Land–atmosphere interactions in the tropics—a review *Hydrol. Earth Syst. Sci.* **23** 4171–97

Gloor M, Brienen R J W, Galbraith D, Feldpausch T R, Schöngart J, Guyot J L, Espinoza J C, Lloyd J and Phillips O L 2013 Intensification of the Amazon hydrological cycle over the last two decades *Geophys. Res. Lett.* **40** 1729–33

Green J K, Berry J, Ciais P, Zhang Y and Gentine P 2020 Amazon rainforest photosynthesis increases in response to atmospheric dryness *Sci. Adv.* **6** eabb7232

Guan K *et al* 2015 Photosynthetic seasonality of global tropical forests constrained by hydroclimate *Nat. Geosci.* **8** 284–9

Hersbach H *et al* 2020 The ERA5 global reanalysis *Q. J. R. Meteorol. Soc.* **146** 1999–2049

Huffman G J, Bolvin D T, Nelkin E J, Wolff D B, Adler R F, Gu G, Hong Y, Bowman K P and Stocker E F 2007 The TRMM multisatellite precipitation analysis (TMPA): quasi-global, multiyear, combined-sensor precipitation estimates at fine scales *J. Hydrometeorol.* **8** 38–55

Jung M, Koirala S, Weber U, Ichii K, Gans F, Camps-Valls G, Papale D, Schwalm C, Tramontana G and Reichstein M 2019 The FLUXCOM ensemble of global land-atmosphere energy fluxes *Sci. Data* **6** 74

Karlsson K G *et al* 2013 CLARA-A1: a cloud, albedo, and radiation dataset from 28 years of global AVHRR data *Atmos. Chem. Phys.* **13** 5351–67

Kent C, Chadwick R and Rowell D P 2015 Understanding uncertainties in future projections of seasonal tropical precipitation *J. Clim.* **28** 4390–413

Knutson T R and Zeng F 2018 Model assessment of observed precipitation trends over land regions: detectable human influences and possible low bias in model trends *J. Clim.* **31** 4617–37

Langenbrunner B, Pritchard M S, Kooperman G J and Randerson J T 2019 Why does Amazon precipitation decrease when tropical forests respond to increasing CO_2? *Earth's Future* **7** 450–68

Lenton T M, Held H, Kriegler E, Hall J W, Lucht W, Rahmstorf S and Schellnhuber H J 2008 Tipping elements in the Earth's climate system *Proc. Natl Acad. Sci.* **105** 1786–93

Levine P A, Randerson J T, Swenson S C and Lawrence D M 2016 Evaluating the strength of the land–atmosphere moisture feedback in Earth system models using satellite observations *Hydrol. Earth Syst. Sci.* **20** 4837–856

Malhi Y, Aragão L E, Galbraith D, Huntingford C, Fisher R, Zelazowski P, Sitch S, McSweeney C and Meir P 2009 Exploring the likelihood and mechanism of a climate-change-induced dieback of the Amazon rainforest *Proc. Natl Acad. Sci.* **106** 20610–5

Marengo J A 2006 On the hydrological cycle of the Amazon Basin: a historical review and current state-of-the-art *Rev. Bras. Meteorol.* **21** 1–19

Marengo J A and Espinoza J C 2016 Extreme seasonal droughts and floods in Amazonia: causes, trends and impacts *Int. J. Climatol.* **36** 1033–50

Marengo J A, Nobre C A, Tomasella J, Oyama M D, Sampaio de Oliveira G, de Oliveira R, Camargo H, Alves L M and Brown I F 2008 The drought of Amazonia in 2005 *J. Clim.* **21** 495–516

Martens B, Miralles D G, Lievens H, van der Schalie R, de Jeu R A, Fernández-Prieto D, Beck H E, Dorigo W A and Verhoest N E 2017 GLEAM v3: satellite-based land

evaporation and root-zone soil moisture *Geosci. Model Dev.* **10** 1903

Miralles D G, Holmes T R H, de Jeu R A M, Gash J H, Meesters A G C A and Dolman A J 2011 Global land-surface evaporation estimated from satellite-based observations *Hydrol. Earth Syst. Sci.* **15** 453–69

Mu Q, Heinsch F A, Zhao M and Running S W 2007 Development of a global evapotranspiration algorithm based on MODIS and global meteorology data *Remote Sens. Environ.* **111** 519–36

Mu Q, Zhao M and Running S W 2011 Improvements to a MODIS global terrestrial evapotranspiration algorithm *Remote Sens. Environ.* **115** 1781–800

Mueller B and Seneviratne S I 2014 Systematic land climate and evapotranspiration biases in CMIP5 simulations *Geophys. Res. Lett.* **41** 128–34

O'Sullivan M *et al* 2020 Climate-driven variability and trends in plant productivity over recent decades based on three global products *Glob. Biogeochem. Cycles* **34** e2020GB006613

Rammig A, Jupp T, Thonicke K, Tietjen B, Heinke J, Ostberg S, Lucht W, Cramer W and Cox P 2010 Estimating the risk of Amazonian forest dieback *New Phytol.* **187** 694–706

Riahi K, Rao S, Krey V, Cho C, Chirkov V, Fischer G, Kindermann G, Nakicenovic N and Rafaj P 2011 RCP 8.5—a scenario of comparatively high greenhouse gas emissions *Clim. Change* **109** 33

Rowell D P, Senior C A, Vellinga M and Graham R J 2016 Can climate projection uncertainty be constrained over Africa using metrics of contemporary performance? *Clim. Change* **134** 621–33

Salati E, Dall'Olio A, Matsui E and Gat J R 1979 Recycling of water in the Amazon basin: an isotopic study *Water Resour. Res.* **15** 1250–8

Seneviratne S I *et al* 2013 Impact of soil moisture-climate feedbacks on CMIP5 projections: first results from the GLACE-CMIP5 experiment *Geophys. Res. Lett.* **40** 5212–7

Sitch S *et al* 2015 Recent trends and drivers of regional sources and sinks of carbon dioxide *Biogeosciences* **12** 653–79

Skinner C B, Poulsen C J, Chadwick R, Diffenbaugh N S and Fiorella R P 2017 The role of plant CO_2 physiological forcing in shaping future daily-scale precipitation *J. Clim.* **30** 2319–40

Sörensson A A and Ruscica R C 2018 Intercomparison and uncertainty assessment of nine evapotranspiration estimates over South America *Water Resour. Res.* **54** 2891–908

Spracklen D V, Arnold S R and Taylor C M 2012 Observations of increased tropical rainfall preceded by air passage over forests *Nature* **489** 282–5

Staal A, Tuinenburg O A, Bosmans J H C, Holmgren M, van Nes E H, Scheffer M, Zemp D C and Dekker S C 2018 Forest-rainfall cascades buffer against drought across the Amazon *Nat. Clim. Change* **8** 539–43

Sun L, Baker J C A, Gloor E, Spracklen D, Boesch H, Somkuti P, Maeda E and Buermann W 2019 Seasonal and inter-annual variation of evapotranspiration in Amazonia based on precipitation, river discharge and gravity anomaly data *Front. Earth Sci.* **7** 1–9

van der Ent R J, Savenije H H, Schaefli B and Steele-Dunne S C 2010 Origin and fate of atmospheric moisture over continents *Water Resour. Res.* **46** 1–12

Wilks D S 2016 'The stippling shows statistically significant grid points': how research results are routinely overstated and overinterpreted, and what to do about it *Bull. Am. Meteorol. Soc.* **97** 2263–73

Wright J S, Fu R, Worden J R, Chakraborty S, Clinton N E, Risi C, Sun Y and Yin L 2017 Rainforest-initiated wet season onset over the southern Amazon *Proc. Natl Acad. Sci.* **114** 8481–6

Yin L, Fu R, Shevliakova E and Dickinson R E 2013 How well can CMIP5 simulate precipitation and its controlling

processes over tropical South America? *Clim. Dyn.*
41 3127–43

York D 1966 Least-squares fitting of a straight line *Can. J. Phys.*
44 1079–86

Zemp D C, Schleussner C-F, Barbosa H M J, Hirota M,
Montade V, Sampaio G, Staal A, Wang-Erlandsson L

and Rammig A 2017 Self-amplified Amazon forest loss due
to vegetation-atmosphere feedbacks *Nat. Commun.* **8** 1–10

Zhang K, Kimball J S, Nemani R R and Running S W 2010 A
continuous satellite-derived global record of land surface
evapotranspiration from 1983 to 2006 *Water Resour. Res.*
46 21